Investigation on the permeability enhancement of Dahebian syncline coal rock in Liupanshui coalfield

Yuanlong Wei[1,2], Lingyun Zhao[1,2,4], Yinlan Fu[1,2,a*], Fuping Zhao[1,2], Wei Liu[2,3], Gang Xiang[1,2], Xuanshi Zhu[3], Xiong Zhang[3,b*]

[1]Key Laboratory of Unconventional Gas Evaluation and Development in Complex Structural Areas, Guiyang 550081, China
[2]Guizhou Institute of Petroleum Exploration and Development Engineering, Guiyang 550081, China
[3]State Key Laboratory of Coal Mine Disaster Dynamics and Control, Chongqing University, Chongqing 400044, China
[4]College of Resources and Environmental Engineering, Guizhou University, Guiyang 550025, China

Abstract: Guizhou Province of Southwest China is abundant in coal mines, including a significant amount of coalbed methane (CBM) resources. However, the development of CBM has not yet achieved major commercial success. The main method of CBM development in Guizhou Province is hydro-fracturing technology, primarily using cluster-well mode. To accurately evaluate the reconstruction effect and permeability enhancement of the typical coal seams of the Dahebian syncline, and to provide a scientific basis for the hydro-fracturing and drainage control of the target coal seams, systematic research was conducted on the Longtan Formation coal seam in Dahebian syncline of Liupanshui coalfield. Firstly, porosity and permeability tests were conducted to analyze the relationship between the permeability of original coal samples and confining pressure. Secondly, uniaxial compressive tests were performed on coal samples with bedding angles of 0° and 90°, respectively, thus to induce splitting cracks or shear cracks in the samples and to simulate the fracturing effect in the coal seam. Thirdly, the permeability of coal after uniaxial compression was measured, and the characteristics of permeability change in fractured/damaged coal samples were analyzed. Finally, the differences in permeability characteristics between original coal samples and those after uniaxial compression were compared. The reconstruction and effects of permeability enhancement of coal were also analyzed by considering the brittleness characteristics of coal seam as well as the distribution of original fissures/cracks/fractures. Furthermore, countermeasures for CBM development that are conducive to on-site fracturing were discussed.

1. Introduction

As an important clean energy source, natural gas plays a crucial role for transiting fossil energy to zero-carbon energy [1-4]. In 2023, China' annual natural gas consumption reached approximately 3945×10^8 m^3, while the production of which was only 2300×10^8 m^3. Due to limitations in proven reserves and conventional natural gas resources exploitation capacity, up to now, China's dependence on foreign countries for natural gas has risen to 41.70%. Therefore, it is of great significance to increase the exploration and development of unconventional natural gas resources so as to promote reform in the national energy landscape [5-6]. The geological resources of unconventional natural gas in China, such as shale gas, coalbed methane (CBM), and tight gas, are substantial. Notably, the geological resources of CBM exceed 30×10^{12} m^3 [7-8]. Currently, China has made significant progress in the exploration and development of shale gas and tight gas [9-11], with new advancements also being made in CBM exploration and development. In 2023, the total CBM production in China amounted to about 117×10^8 m^3, accounting for approximately 5% of the domestic natural gas supply, thus serving as an important supplement to the domestic natural gas supply.

Nevertheless, the development of CBM in many coal mines of China still far behinds the planning. Taking Guizhou Province as an example, the majority of coal seams belong to soft coal beds with low porosity and permeability in complex structural areas [13-15]. Despite the geological resources of CBM in Guizhou province exceeding 3×10^{12} m^3 [16], the annual production of CBM is still as low as 4×10^8 m^3. The production of CBM in Guizhou Province significantly lags behind its vast resources, posing challenges not only for regional gas supply but also presenting a substantial risk for coal mine safety production. In consideration of the low porosity and permeability characteristics of coal seams both domestically and internationally, hydro-fracturing remains the primary method for reconstructing the coal reservoirs [17-18]. hydro-fracturing involves using high-pressure prefluid to create cracks in coal seams that connect with natural fissures/fractures, and sand-carrying fluid to drive proppant into these fractures, thus providing channels for methane gas migration [19-20].

The success of a coal seam's yield depends on the effectiveness of the reconstruction and the degree of permeability increase, specially whether sufficient cracks

Corresponding author's email: [a]*Liberty5258@163.com; [b*] alzhangxiong@163.com

can be formed. Scholars from both domestic and international areas primarily focus on the impact of rock breaking mechanism, fracturing fluids, and fracturing technology on coal seam fractures. The selection of fracturing fluid is important in ensuring fracturing effect and long-term conductivity. In order to minimize reservoir damage, low viscosity water-based fracturing fluids are typically utilized in coal seams. The research on fracturing fluids mainly encompasses the application of hydraulic fracturing in the early stages of CBM development, which proved successfully in the Black Warrior Basin in the United states [21]. Additionally, as early as 1995, Jin et al. [22] demonstrated the feasibility of hydro-fracturing in CBM development by using water-based fracturing fluid and achieved a high daily production of f 5,000 m^3 per well in the Jincheng anthracite coal seams. Fredd et al. [23] highlighted the superior cleaning effects of polymer-free fracturing fluids in unconventional natural gas wells. In order to improve the coal seam fracturing, some scholars have introduced pulsating hydro-fracturing technology. Zhai et al. [24] demonstrated that pulsating hydro-fracturing has a more pronounced pressure relief and reflection enhancement effect compared to ordinary hydraulic fracturing, leading to greatly improvements in gas extraction concentration and flow rate in boreholes. Huang et al. [25] conducted a systematic study on the effects and mechanisms of three water-based fracturing fluids (slippery water, crosslinked guar gum, and viscoelastic surfactant fracturing fluid) on coal seam gas flow. Liu et al. [20] investigated the sand-carrying capacity of fracturing fluid and the deposition patterns of quartz sand in simulated fracturing cracks in coal seam. In addition, the use of fracturing fluid as an external liquid may lead to reservoir damage while causing fractures in the reservoirs. Some scholars have also investigated the adverse effects of fracturing fluid on coal seam. Duan et al. [26] demonstrated that fracturing has obvious implications for the transformation of CBM reservoirs and imposes substantial limitations on the long-term and efficient discharge and production of CBM. It is essential to rigorously control the construction technology of fracturing and laws governing pressure reduction in order to effectively enhance discharge and production efficiency.

Currently, the theories and technologies related to CBM development are still largely based on shale gas development. This involves creating numerous cracks in the coal seam by injecting high-pressure sand-carrying fracturing fluid, artificially improving reservoir permeability and providing channels for gas and water production. However, it is important to consider the nature of the coal seams themselves during CBM development. The coal seams have low strength, unstable state, developed joints and fractures, and sometimes they are broken or even crushed in structure.

The primary focus remains on the objective of "pressure relief and permeability enhancement" in the coal seams. In line with this, it is particularly important to conduct evolutions of permeability enhancement and hydro-fracturing effects of coal seam before and after fracturing, thus to guide the development of CBM. Wang et al. [27] conducted a study on the change and distribution laws of coal seam permeability around hydraulic punching boreholes, and determined the pressure relief range and gas pressure distribution around the borehole. Tu et al. [28] utilized RFPA2D-Gasflow software to analyze the mining fracture development and stress distribution characteristics of overburden coal rock following pressure relief mining, as well as the resulting anti-reflection effect on pressure relieved coal seam. Their findings indicated that during pressure relief mining, there was an increase in gas permeability coefficient by about 200 times. Feng et al. [29] carried out experiments on the evolution law of permeability in the "three soft" coal seams, focusing on the change of coal structure and stress. They found that the permeability of soft coal was greatly increased after pressure relief. Xue et al. [30] studied the impacts of gas fracturing on coal seam fracture characteristics and gas extraction effectiveness using a multi-physical field model. Cai et al. [31] discussed the principle, advantages, disadvantages, and technological characteristics of liquified-CO_2 fracturing technology. They compared the steps and effects of liquified-CO_2 construction, and recommended targeted use of this technology in CBM fracturing. The aforementioned research primarily focused on coal seams with relatively favorable development conditions in China or gas extraction in underground working faces. However, there are significant differences in geological conditions and reservoir conditions when compared to surface fracturing exploitation of CBM in Guizhou complex structural area.

In order to investigate the effect of fractured cracks on permeability enhancement in coal reservoirs and provide a basis for optimizing fracturing construction technology and parameters, this paper selected raw coal from the Dahebian syncline 11# coal seam in the Liupanshui coalfield as the research object. Raw coal samples with bedding angles of 0° and 90° were prepared. At first, porosity and permeability characteristics of the coal samples under different confining pressures were tested. Subsequently, uniaxial compression tests were conducted on coal samples to simulate the formation of cracks by inducing tensile or shear cracks in the samples. Finally, permeability tests of the fractured samples under different confining pressures were carried out, and the increase in permeability effect was analyzed along with discussing countermeasures for field development. This study can serve as a theoretical reference for hydro-fracturing designing and effectiveness evaluation of similar coal seams in Liupanshui or similar coalfields.

2. Materials and methods

2.1 Geological Conditions and Core Extraction

The CBM area in Dahebian syncline methane area of Liupanshui coalfield of Longtan Formation of Upper Permian in Guizhou province belongs to the middle section of the west wing of Dahebian syncline in the northwest tectonic deformation area of Weining in the Yangtze continental block (level I), Qianbei uplift (level II) and Liupanshui fault depression (level III). After coal formation in Dahebian syncline, it was invaded successively by Hualisi movement, Indosinian movement

and Yanshan movement, which destroyed the original state of the coalfield. Controlled by Yadu-Ziyun tectonic belt and the northwest-westerly fault zone of Weishui, the main tectonic line in the syncline is NWW-SEE.

There are seven main coal seams in the working area, namely 1#, 4#, 7#, 8#, 11#, 12# and 13# coal seam, respectively. Among them, 1#, 7#, 11#, 12# and 13# are the minerable coal seams in the whole area, and 4# and 8# are most minerable coal seams. The 11# coal seam is the largest and most gas-bearing coal seam in the working area, and it is also the sampling coal seam in this paper. The 11# coal seam is located in the middle part of the second stage of Longtan Formation (P_3l^2), approximately 29.4-45.05 m above the B2 marker layer and 26.45-41.39 m below the B3 marker layer. It is estimated at a depth of 800-900 m, with a thickness ranging from 4.73-7.02 m and an average of 5.66 m, making it the primary minerable coal seam with stable distribution through the whole area. The structure of the 11# coal seam consists of both primary and fragment structures, with obvious bedding structure and relatively developed original fissures/cracks as well as good gas content, ensuring it a key layer for potential CBM development in the working area.

When hydro-fracturingis applied to a coal seam, numerous artificial cracks are created, primarily consisting of tensile fractures accompanied by some shear fractures. The change in permeability before and after fracturing serves as an important indicator for evaluating fracturing effectiveness and provide a fundamental reference for on-site fracturing fluids discharge design, proppant selection, fracturing construction optimization, and drainage gas recovery control. Based on the changes in coal permeability, this paper will proceed with research as follows:

(1) Test and analyze the porosity and permeability of the coal samples. The porosity of original coal samples will be measured using gas expansion method, followed by testing the permeability while increasing and decreasing confining pressure (2→10→2 MPa) to obtain the permeability evolution characteristics.

(2) Obtain coal samples with cracks. It is difficult to obtain tensile or shear cracks through laboratory fracturing, so uniaxial compression tests will be conducted on 0° and 90° coal samples to induce a certain amount of splitting cracks or shear cracks within coal sample. The selection of 90° samples is to prepare cracks parallel to the bedding direction, while the selection of 0° samples is to prepare cracks perpendicular to or intersecting the bedding plane (probably shear-slipping cracks).

(3) Test the permeability of coal samples those contain cracks. The damaged coal sample from uniaxial compression already contains a certain number of tensile cracks or shear cracks, and then undergoes a permeability test while pressurizing and depressurizing the confining pressure (2→10→2 MPa) to obtain the permeability characteristics of the damaged coal sample, thus to investigate its effect on improving the permeability of coal seam.

(4) Evaluate the effect on permeability enhancement in coal sample and discuss CBM development. The test results will be processed and analyzed, discussing various angles regarding permeability enhancement for different angled coal samples, as well as proposing development measures and suggestions for site application.

2.2 Test Theory and Scheme

Calculation formula of coal sample permeability:

$$K = \frac{2P_0 Q\mu L}{A(P_1^2 - P_2^2)} \tag{1}$$

Where, K is the permeability, mD; P_0 is the atmospheric pressure, which is 0.1 MPa; Q is the gas flow, ml/s; μ is the gas viscosity, mPa·s; L is the core length, m; A is the cross-sectional area of sample, m^2; P_1 is the inlet gas pressure, MPa; P_2 is the outlet gas pressure, which equals the atmosphere pressure.

Calculation formula of coal sample porosity (gas expansion method):

$$\varphi = \frac{1\text{-}[P_2(V_1 + V_2)\text{-}V_1P_1]}{P_2(V_f + V_s)} \tag{2}$$

Where, φ is the porosity of the sample, %; V_f is the total volume of sample, cm3; V_s is the solid phase volume of rock, cm3; V_1 is the standard chamber volume, cm3; V is the volume of the gripper connected to it, cm3; P_1 is the gas pressure before equilibrium, MPa; P_2 is the gas pressure after equilibrium, MPa.

The permeability and porosity testing equipment were referred to as the LW-1 automatic permeability, which was development by Chongqing University. Detailed information about the equipment introduction and operation flow can be found in the references [32-33].

2.3 Preparation of Coal Samples

Considering the presence of numerous original fissures/cracks and generally low strength of coal rock, all coal samples were obtained through wire cutting. As depicted in Fig. 1, a total of ten samples were prepared for this study, with four being 0° samples (parallel to the bedding direction) for analyzing the permeation effect of vertical cracks, and six being 90° samples (vertical to the bedding direction) for analyzing the permeation effect of cracks along the bedding direction. Following the uniaxial compression test, the transverse size of the samples will increase. To fit the sample into the permeability equipment's test holder, its diameter is controlled below 46 mm. The specific information regarding each sample is presented in Table 1, "0" indicates a bedding angle of 0° and "90" indicates a bedding angle of 90°. Porosity serves as a fundamental parameter. Initially, the porosity tests were conducted as shown in Table 1, before testing permeability during increasing and decreasing confining pressure. In Chapter 4, the results will be compared with those from permeability tests on coal samples after uniaxial

compression tests.

The initial porosity of coal samples ranges from 2.59-9.39%, with an average of 7.085%. In addition to the obvious bedding, original fissures/cracks are also developed in the coal samples, and fissures/cracks with different sizes and orientations crisscross the surface. Usually, the development of original fissures/cracks is a favorable condition for hydraulic fracturing. During hydraulic fracture propagation, the bedding surfaces and original fissures/cracks will jointly affect the reconstruction effects in coal seam, leading to crack migration, turning, and bifurcation. This is conducive to the formation of a complex volume crack network and can also create conditions for subsequent drainage and gas desorption migration. However, it should be noted that according to the original fissures/cracks and porosity test results, there is a significant variation in the porosity of coal samples.

The porosity of Sample 90-2 is the lowest, at only 2.59%. The original fissures/cracks on the surface of this coal sample are not well developed, and the connectivity of them is also weak, indicating good sample integrity. In contrast, Sample 0-04 has the highest porosity at 9.39%, with a fracture zone running almost through the axial direction of the sample ends and several groups of intersecring original fissures/cracks developed. This also demonstrated that bedding planes and original fissures/cracks in coal seams are random and heterogeneous, posing challenges for accurate prediction of fracture networks. These factors also contribute to significant differences in CBM production between adjacent wells in Guizhou province.

(a) All coal samples for research

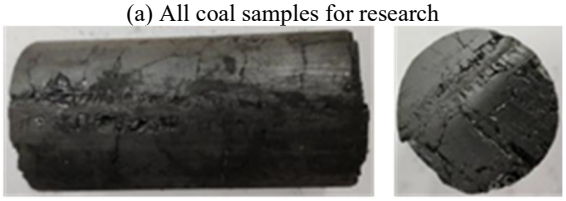

(b) 0° representative coal sample

(c) 90° representative coal sample

Fig. 1. Coal rock samples used for research

Table 1. Petro-physical parameters of coal samples

Sample No.	Size/mm		Mass	Density	Orginal porosity
	Diameter	Length	/g	/(g·cm^3)	%
0-01	45.53	92.30	198.63	1.32	8.29
0-02	45.95	92.29	199.25	1.30	8.98
0-03	45.88	92.46	198.97	1.30	8.76
0-04	45.92	92.26	197.02	1.29	9.39
90-01	45.80	92.29	197.57	1.30	6.41
90-02	45.36	92.33	196.80	1.32	2.59
90-03	45.47	92.28	204.49	1.36	6.53
90-04	45.55	92.28	195.84	1.30	8.03
90-05	45.61	92.25	196.08	1.30	6.32
90-06	45.57	92.32	201.19	1.34	5.55

3. Results and discussion

3.1 Uniaxial compression test

After conducting the porosity and permeability tests, uniaxial compression tests were performed on the coal samples listed in Table 1. To prevent the coal samples from collapsing into fragments after reaching peak pressure, which could impact subsequent permeability testing, the lateral surface of each sample was tightly wrapped with transparent heat shrinkable tubes before testing. Additionally, a low displacement loading rate (0.02 mm/s) was utilized during loading. Through the test, axial load, axial displacement, and circumferential displacement were recorded to calculate axial stress, axial strain, circumferential strain, and volumetric strain.

Four representative uniaxial compression stress-strain curves were selected as shown in Fig. 2.

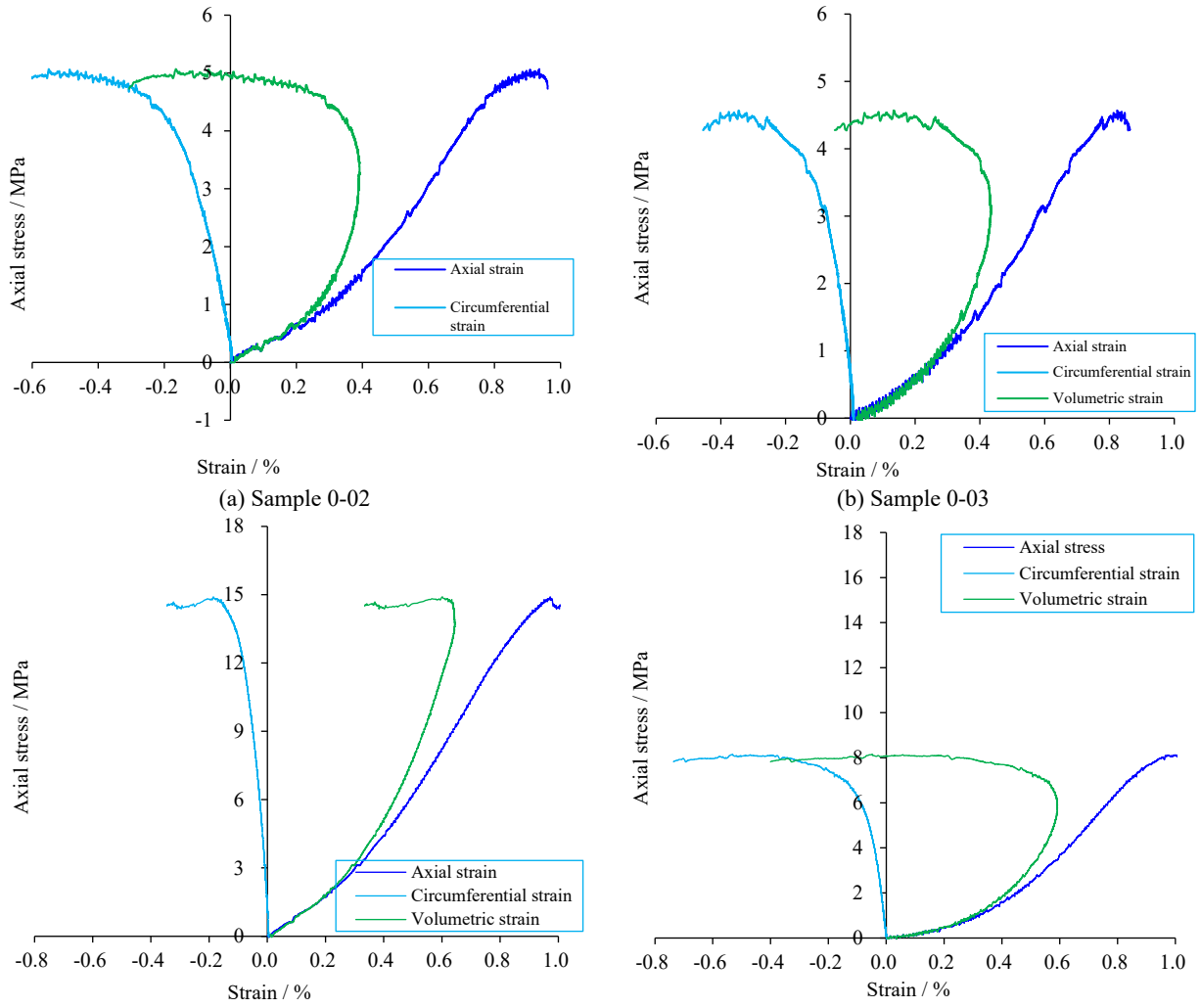

Fig. 2. Typical stress-strain curves of uniaxial compression tests for 0° and 90° coal samples

The results of uniaxial compression tests are presented in Table 2.

The uniaxial compressive strength of the 0° coal samples ranges from 2.943-4.736 MPa, with an average of 4.448 MPa (Protodyakonov's coefficient f=0.4448). The overall strength is low, indicating that it belongs to a soft coal seam. The peak strain ranges from 0.725 to 1.064%, with an average of 0.887%. This suggests a prolonged compaction stage and larger peak strain. The sharp zigzag fluctuation at the peak of the stress-strain curve indicates significant shear slip on the fracture surface. Three samples exhibited shear failure or shear-dilatation failure, while only Sample 0-03 showed splitting-shear failure, with the lowest peak strain among all samples.

The uniaxial compressive strength of the 90° coal samples is between 6.184-15.162 MPa, with an average of 9.911 MPa (Protodyakonov's coefficient f=0.991), which is higher than that of the 0° coal samples, but it still belongs to the category of soft coal seam. The peak strain range is 0.731-1.063%, and the average strain is 0.888%, similar to the 0° samples. When loading to the peak failure, the stress-strain curve is smooth, and the peak failure results in rupture, indicating more obvious brittleness in this stage.

The coal samples can be categorized into two primary modes: splitting failure and shear failure. Upon comparing the pictures of a coal sample (Fig. 1), it is evident that when there are more original fissures/cracks with small angles or parallel to the loading direction, the likelihood of splitting failure mode occurring in this sample increases. Conversely, when there are more original fissures/cracks with large angles or even perpendicular to the loading direction, the coal sample is more likely to be damaged by shearing or dilatation. The density, occurrence, and shape of original fissures/cracks significantly influence the failure of coal sample. It is easier for a splitting tensile fracture plane to form along the bedding direction, while it is easier for shear or dilatation fracture surface to form along a direction vertical to the bedding

Table 2. Uniaxial compression test results and failure description of coal samples

Bedding angle	Sample No.	Peak stress /MPa	Peak strain /%	Volumetric strain/%	Coal sample characteristics	Fracture characteristics
0°	0-01	2.943	1.064	-0.452	Many original fissures/cracks	Many peak points, shear failure

	0-02	5.269	0.935	-0.165	Many original fissures/cracks	Many peak points, dilatant failure
	0-03	4.736	0.725	-0.111	A few original fissures/cracks	Splitting-shear failure
	0-04	4.845	0.824	0.135	Many original fissures/cracks	Splitting-dilatant failure
Average	/	4.448	0.887	-0.148		
90°	90-02	15.162	0.935	-0.165	Many original fissures/cracks	Splitting failure
	90-03	10.769	0.731	0.127	Good integrity, a few original fissures/cracks	Splitting failure
	90-04	9.086	0.739	0.094	Some original fissures/cracks	Splitting-shear
	90-05	8.134	1.063	-0.341	Many original fissures/cracks	Dilatancy failure
	90-06	6.184	0.973	-0.090	Many original fissures/cracks	Shear failure dominantly
Average	/	9.911	0.888	-0.375		

3.2 Test Results of Permeability

Before and after conducting uniaxial compression tests, the permeability of coal samples was individually tested under identical conditions. The confining pressure was incrementally increased and then decreased in steps. The incremental increase in confining pressure followed a sequence of 2 → 4 → 6 → 8 → 10 MPa, while the decremental decrease followed a sequence of 10 → 8 → 6 → 4 → 2 MPa, with an inlet gas pressure of 0.4 MPa. Upon reaching each set confining pressure, three gas flow tests were conducted after the flow rate stabilized, and the permeability under the corresponding confining pressure was calculated based on its average value. The states of coal samples before and after uniaxial compression test are referred to as "Original state" and "After-fracture," respectively. The permeability for coal samples before and after fracture were plotted on the same coordinate system for comparison purposes. All test results are presented in Fig. 3 below.

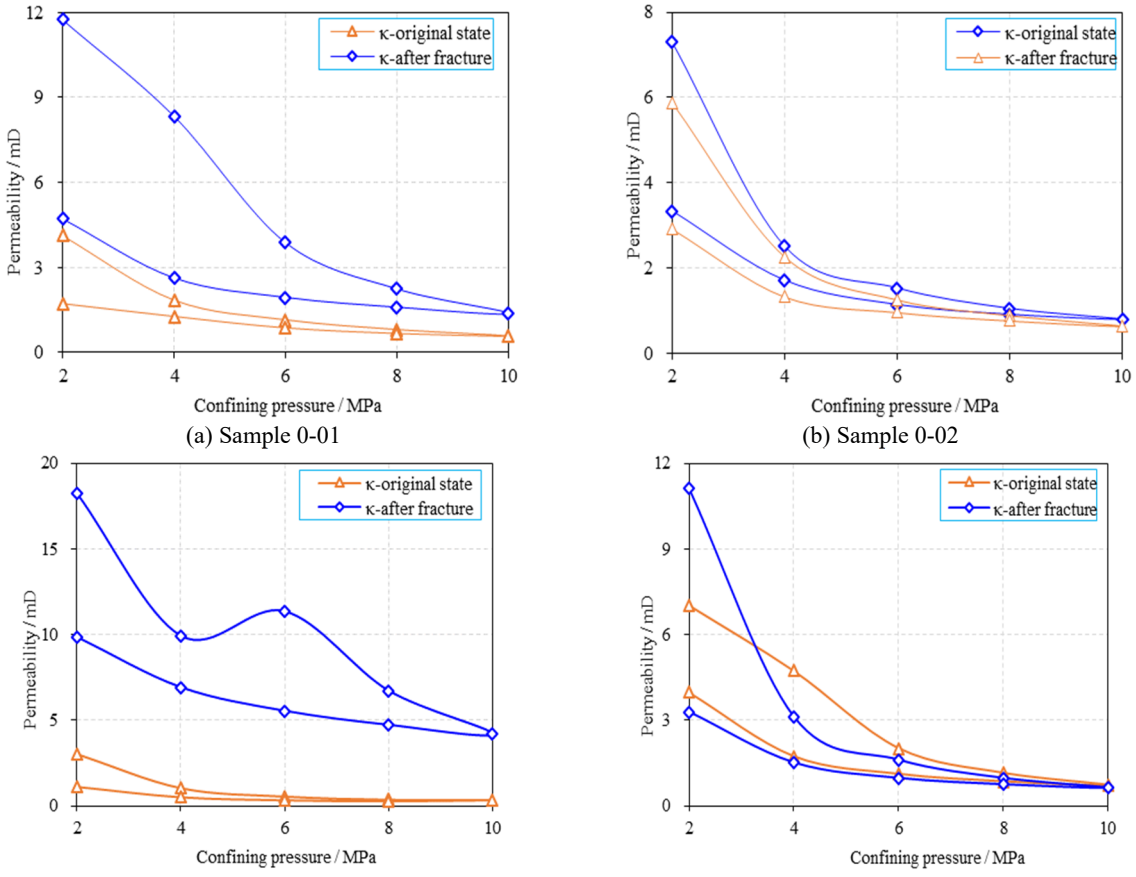

(a) Sample 0-01 (b) Sample 0-02

(c) Sample 0-03 (d) Sample 0-04

Fig. 3. Permeability test results of raw coal samples before and after fracture (normalized treatment)

3.2.1 Test Result of 0° Samples

For the coal samples in their original state, during the step-increasing stage of confining pressure, the permeability at a confining pressure of 2 MPa ranges from 3.014 to 7.295 mD, with an average of 5.368 mD. This reflects the permeability along the bedding direction when the fissures/fractures have not been completely closed after pressure relief. As the confining pressure increases to 10 MPa, the permeability ranges within 0.348-0.79 mD, with an average of 0.606 mD, representing the permeability of coal sample fissures/fractures along the bedding direction when they are well compacted. The change trend of

permeability with confining pressure indicates that as confining pressure increases, there is a rapid decrease in permeability and when reaching high levels (8-10 MPa), this attenuation gradually slows down. It can be considered that under a confining pressure of 10 MPa, the permeability is close to that of the original coal seam's permeability before any changes occurred due to increased pressures and compaction processes.

The average permeability of the 0° coal samples under 10 MPa is only 0.606 mD, indicating that it belongs to a low-permeability coal seam and requires artificial reconstruction. During the stage of confining pressure reduction, the permeability of the coal samples is consistently lower than that of the corresponding confining pressure increasing section. However, when the confining pressure is higher (10 → 8 → 6 MPa), the permeability of the depressurizing section approaches that of the confining pressure increasing section, as most fissures/fractures in the coal sample have been compacted or closed under high confining pressure. As the confining pressure is further reduced to 4 MPa and 2 MPa, it becomes evident that the permeability of the depressurization section is significantly lower than that of the pressurization section. This can be attributed to coal rock being a typical soft rock, with internal deformation and fissure/fracture closure characterized by plastic deformation during loading processes. Consequently, corresponding deformation and fissure/fracture widths cannot be fully recovered during the stages of confining pressure release.

For the coal sample subjected to uniaxial compression test (after fracture), during the confining pressure rising stage, the permeability range corresponding to a confining pressure of 2 MPa increases to 5.689-18.224 mD, with an average of 11.735 mD. This reflects the permeability characteristics of the coal sample after cracks and damage have formed, with the permeability being only 2.186 times that of the original stage permeability of the coal samples. As the confining pressure rises to 10 MPa, the corresponding permeability ranges from 0.622-4.181 mD, with an average of 1.705 mD, indicating that the permeability of the coal sample after fracture is now 2.815 times that of its original state. However, in the pressure relief stage, it is observed that the permeability of the coal sample is consistently lower than that during the pressure rising stage and this difference becomes greater as confining pressure decreases. The formation of cracks and damage in a coal sample leads to closure within it which results in plastic deformation and subsequently causes a decrease in its permeability.

3.2.2 Test Results of 90° Sample

Under the original state, the permeability of the coal sample ranges from 0.981 to 11.352 mD under a confining pressure of 2 MPa in the confining pressure rising section, with an average of 3.225 mD representing the permeability of the coal sample in the vertical bedding direction after pressure release. However, this value is still lower than that in the parallel bedding direction. When the confining pressure rises to 10 MPa, the corresponding permeability ranges within 0.044-4.907 mD, with an average of 0.931 mD representing the permeability of the coal sample in a direction perpendicular to the bedding plane after compaction. From observing changes in permeability with confining pressure, it can be seen that there is a faster decrease in permeability compared to that observed for samples at a 0° angle.

However, when the confining pressure reaches 4-6 MPa, the permeability attenuation becomes extremely slow and even stable. At a confining pressure of 10 MPa, the average permeability of the coal sample is only 0.931 mD, indicating low permeability. Therefore, it is necessary to reconstruct the coal seam in order to achieve gas production. During the stage of confining pressure reduction, the permeability of the coal sample consistently remains lower than that during corresponding stages of increasing confining pressure. This behavior is similar to that observed in samples at 0° angle and does not require further elaboration for comparison purposes.

For the coal sample that has undergone a uniaxial compression test (after fracture), the permeability of the coal sample at the pressure rising section corresponding to a confining pressure of 2 MPa has increased to a range of 1.815-22.812 mD, with an average of 7.377 mD. This reflects the permeability characteristics of the coal sample along the bedding direction after fracture formation, but this value is only 2.288 times that of the sample in its original state (before fracture). When the confining pressure rises to 10 MPa, the corresponding permeability ranges within 0.129-9.784 mD, with an average of 1.889 mD, which represents the permeability of the sample after being compacted along the bedding direction after fracture, but is only 2.029 times that of sample in its original state. However, during the release stage of confining pressure, the permeability of the sample is consistently lower than that during the pressure rising phase. This difference becomes increasingly pronounced as the confining pressure decreases. After fracturing, the closure of cracks in the sample results in plastic deformation and a subsequent decrease in permeability. Similar to 0° samples, it is challenging to reopen these cracks after reducing the confining pressure, leading to a significant disparity in permeability between increasing and decreasing confining pressures. The difficulty in reopening fractures after pressure reduction results in a notable contrast in permeability between the rising and decreasing sections of the confining pressure [34-35].

Fig. 4 displays the test results for all 90° samples.

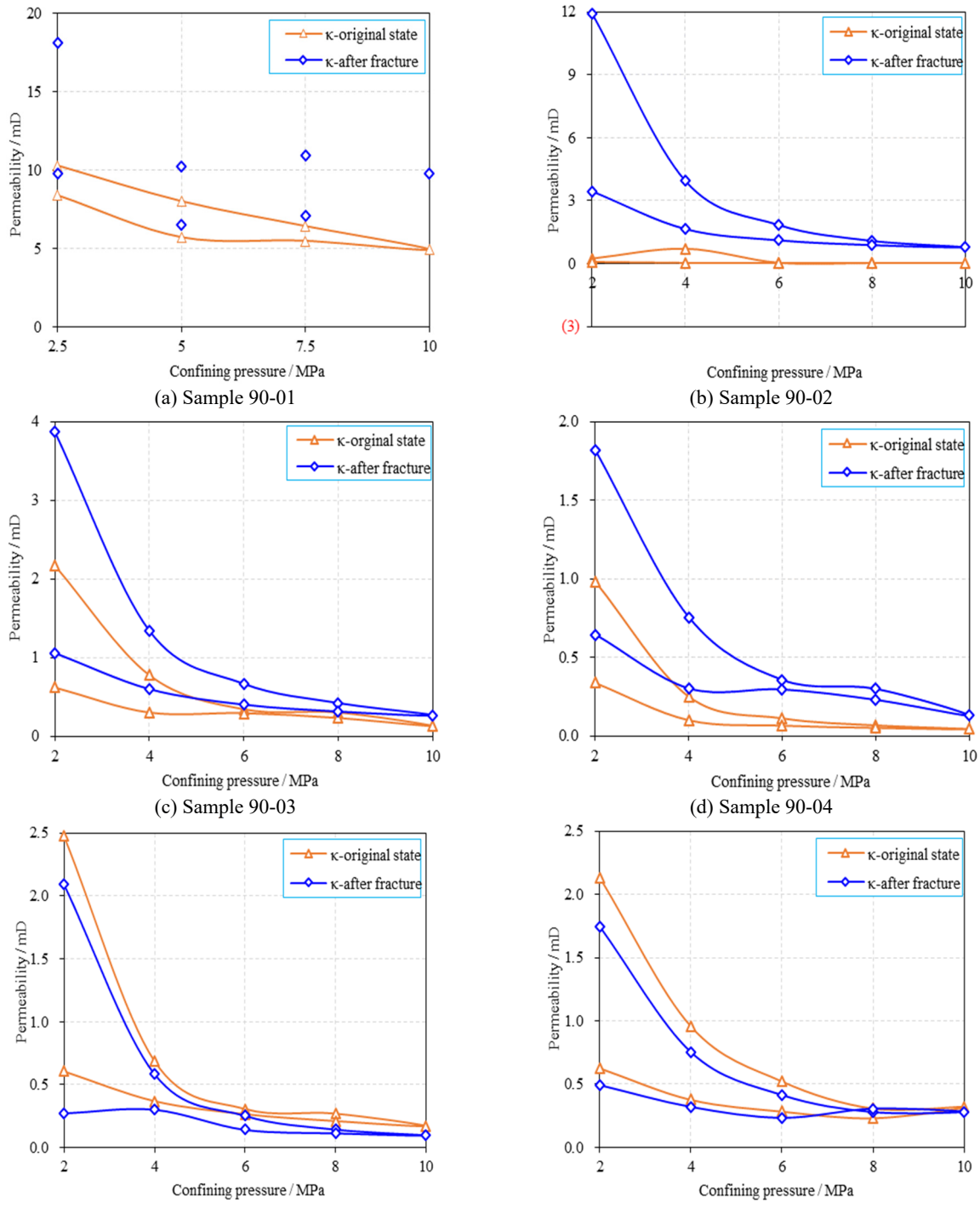

Fig. 4. Permeability test results of 90° coal samples before and after fracture

On the contrary, at the same confining pressure of 2 MPa, the permeability of the 0° samples is higher than that of the 90° samples. This indicates that the permeability along the bedding direction is greater than that in the vertical bedding direction. However, the permeability along the vertical bedding direction reaches 60% of the permeability along the bedding direction, and there is not a significant difference between them. This suggests that the bedding effect is weakened by a large number of original fissures/cracks. When the confining pressure is increased to 10 MPa, it can be observed that the permeability of 0° samples (0.606 mD) is lower than that of 90° samples (0.901 mD). This reflects a stronger stress sensitivity of fissures/cracks along with bedding direction and their tendency to compact more easily. Conversely, there is weaker stress sensitivity for fissures/cracks perpendicular to the bedding direction.

3.3 Analysis of Permeability Enhancement Effect

Under the same confining pressure, the ratio of permeability of the coal sample in the original state to that after fracture state is defined as the permeability increase rate:

$$\eta = \frac{K_{\text{after}}}{K_{\text{before}}} \quad (3)$$

Where, η represents the permeability increase rate, times; K_{before} and K_{after} respectively refer to the permeability of coal sample under the same confining pressure before/after fracture, mD. η >1 indicates a positive permeability enhancement effect, while η < 1 suggests a negative permeability enhancement effect. The introduction of permeability increase rate serves as a normalization of permeability, taking into account the significant variations among individual coal samples and their initial permeabilities. This facilitates an analysis of the overall impact on permeability enhancement. The calculation results for the permeability increase rate of all coal samples in both increasing and decreasing confining pressure sections are presented in Table 3, considering that the permeability test was conducted on original state and fractured coal samples.

Table 3. Permeability increase rate during the sections of increasing and decreasing confining pressure

Comparison	η in confining pressure increasing section		η in confining pressure decreasing section		Mean value of η
Sample No.	Range	Average	Range	Average	
0-01	2.391-4.522	3.185	2.071-2.397	2.37	2.821
0-02	0.805-0.905	0.841	0.777-0.847	0.831	0.838
0-03	6.047-20.694	13.372	8.839-16.939	13.581	13.637
0-04	0.798-1.580	0.952	0.828-0.880	0.867	0.913
Average of 0°	/	4.588	/	4.412	4.552
90-01	1.107-1.994	1.536	1.139-1.997	1.434	1.492
90-02	5.533-63.109	46.572	49.236-72.047	60.371	53.462
90-03	1.394-2.041	1.779	1.347-2.041	1.690	1.700
90-04	1.850-4.369	3.059	1.908-4.440	3.327	3.224
90-05	0.537-0.852	0.727	0.449-0.819	0.585	0.665
90-06	0.784-0.893	0.830	0.781-1.302	0.920	0.876
Average of 90°	/	9.084	/	11.388	10.237

3.3.1 Permeability enhancement of 0° coal samples

As shown in Table 3 above, it is evident that there is a significant increase in permeability among the coal samples. The permeability increase rate during the confining pressure increment ranges from 0.798 to 20.694 times, with an average value of 4.588 times, indicating effective but not ideal permeability enhancement. During the step-decreasing confining pressure stage, the permeability increase rate ranges from 0.777 to 16.939 times, with an average value of 4.412 times. It is important to note that despite the occurange of new cracks and damage to the coal samples as a result of uniaxial compression testing, there is still evidence of "Negative permeability enhancement (η<1)". This suggests that while mechanical loading has caused internal damage to the sample, it has had an adverse effect on its permeability. Further analysis will be conducted in conjunction with damage assessment later.

The permeability of Sample 0-3 is the highest, with η equaling 13.372 in the confining pressure rising section, and η equaling 13.581 in the confining pressure dropping section. This coal sample contains numerous small original fissures/cracks, several veins, and a main fracture zone almost perpendicular to the axis (2-3 mm in width, as shown in Fig. 1). Although the entire sample appears intact, the original fissures/cracks and fracture zone are slightly inclined to the axial direction, and the fracture zone penetrates the sample in the axial direction, which are beneficial for forming gas seepage channels through the sample. In the uniaxial compression test, the sample exhibited splitting-shear failure, further connecting intersecting fissures and forming favorable channels for gas seepage. The permeability increase rate of coal sample 0-02 is the lowest (η=0.841 in the confining pressure increasing section, and η=0.831 in the confining pressure decreasing section). Although the initial porosity of this coal sample reaches 8.98% and it contains a large number of original fissures/cracks with large openings, the inclined angle between the most fissures and the axial direction exceeds 45° or is almost perpendicular to the axial direction. These favorable fissures/cracks in this coal sample are not developed, and there is poor connectivity among them. As a result, it is difficult to form an effective gas permeation channel in this sample. Additionally, it is very challenging to establish an effective gas permeation path in this type of sample. The original fissures/cracks in this coal sample are prone to shear slip failure after being subjected to axial compression, but they do not easily form cracks with small angles or parallel to the axis. Furthermore, due to axial compression and end effect, there may also be partial closure of fissures/cracks at each end.

Therefore, despite the presence of shear cracks in the coal sample following uniaxial compression, it is difficult to create crack channels conductive to gas seepage. The porosity of the two coal samples is approaching (Table 1), and their stress-strain curves also exhibit similarities (Fig. 2). However, due to variations in development degree, occurrence, and distribution of original fissures/cracks in these two coal samples (Fig. 5), there exists a notable disparity between the “positive permeability increase" observed in Sample 0-3 and the "negative permeability increase" observed in Sample 0-2.

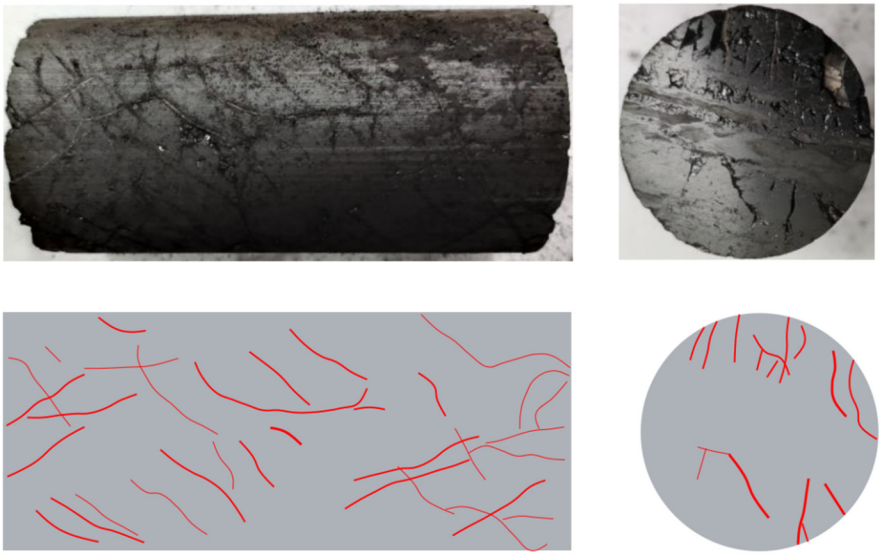

(a) Positive permeability enhancement sample (0-3) and descriptions of original fissures/cracks

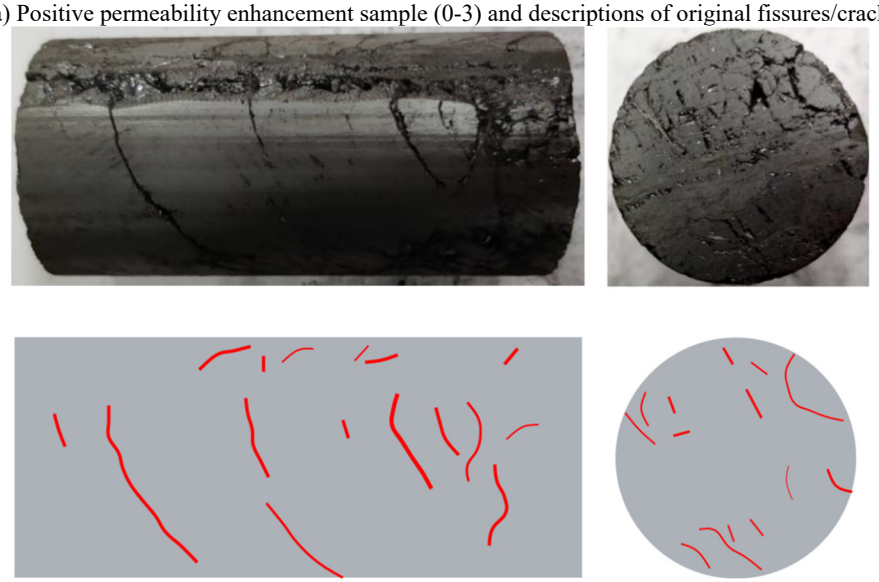

(b) Negative permeability enhancement sample (0-2) and descriptions of original fissures/cracks

Fig. 5. 0° coal samples with negative permeability enhancement and description original fissures/cracks

3.3.2 Permeability Enhancement of 90° Coal Samples

In the section of increasing confining pressure, the permeability increases rate ranges from 0.537 to 63.109 times, with an average of 9.084 times, which is approximately one order of magnitude and significantly higher than that of the 0° coal samples. In the section of decreasing confining pressure, the permeability increase rate is between 0.449 and 72.047 times, with an average of 11.388 times. Generally, the permeability increase rate of the 90° samples in the confining pressure rising section is lower than that in the confining pressure reduction section, resulting in an overall permeability increase rate of approximately 10.237 times. It should be noted that the stress-strain curve of the 90° coal samples under uniaxial compression is smoother, exhibiting higher strength and more obvious brittleness compared to other angles tested. Additionally, more splitting cracks or through cracks are formed during loading process for these samples, leading to a more pronounced overall permeability enhancement effect. However, within the group of 90° coal samples, there are also two instances where "negative permeability increase" occurs despite having more original fissures/cracks present; this can be attributed to shear fracture behavior dominating during uniaxial compression testing without formation of a penetrating fracture plane, resulting in "negative increased permeability".

In all permeability tests, Sample 90-2 exhibits the highest permeability increase rate (46.572 times in the pressuring rising section and 60.371 times in the depressurization section). Despite its initial porosity of only 2.59%, this sample demonstrates good integrity, relatively high peak strength (10.769 MPa), and low peak strain (0.731%). As depicted in Fig. 6(a), typical splitting failure has resulted in numerous cracks parallel to the splitting failure characteristics. This observation underscores that samples with higher brittleness are more likely to generate dominant permeation channels. Even without original fissures/cracks, coal seams with good brittleness may develop penetrating cracks in the vertical bedding direction, thereby enhancing fracturing within

the coal seams. Conversely, Sample 90-5 displays the lowest increase rate in permeability (0.727 times in the pressure rising section and 0.585 times in the depressurization section), despite having an initial porosity of 6.32%. Although this coal sample contains numerous original fissures/cracks predominantly perpendicular to the axial direction, their poor connectivity diminishes their potential as dominant pathways for gas seepage channels formation (Fig. 6(b)). Additionally, this sample undergoes a relatively prolonged compaction stage and reaches a maximum peak strain of 1.063% during uniaxial compression testing, which indicates weak brittleness but strong ductility properties.

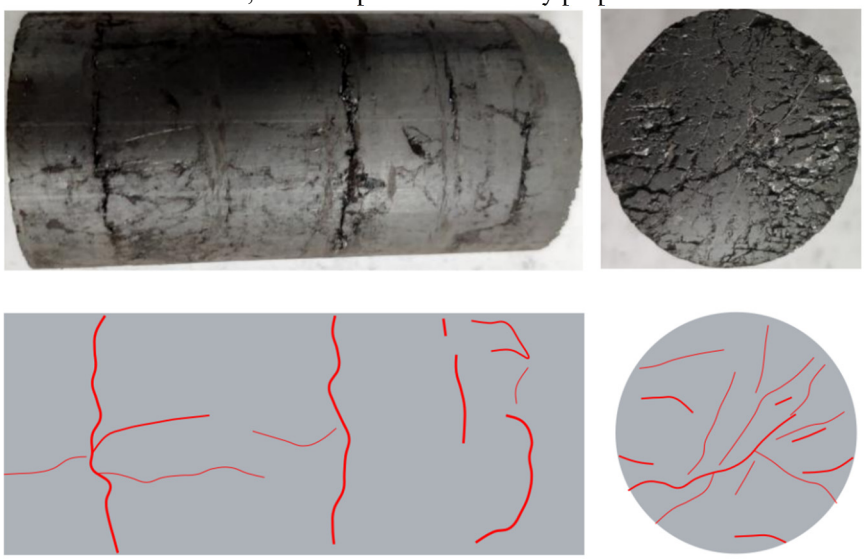

(a) Positive permeability enhancement sample (90-2) and descriptions of original fissures/cracks

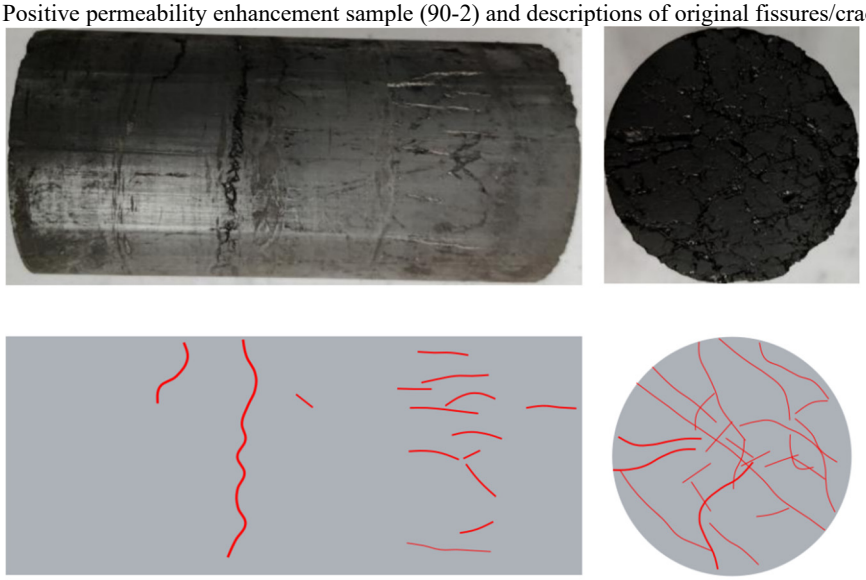

(b) Negative permeability enhancement sample (90-5) and descriptions of original fissures/cracks

Fig. 6. 90° coal samples with opposite permeability enhancement and description original fissures/cracks

3.4 Discussion on CBM Development Countermeasures

The permeability enhancement results of 0° and 90° coal samples indicate the importance of considering the relationship between original fissures/cracks and potential penetration channels, even when a large number of original fissures/cracks or fractures exist. Fissures or cracks that contribute to the formation of gas seepage cracks are termed 'Favorable original fissures/cracks', while others are referred to as 'Inferior original fissures/cracks'. The brittleness of the coal sample significantly influences permeability enhancement effect, particularly in cases of weak brittleness. Weakly brittle coal seams may result in rapid closure of the hydro-fracturing induced cracks, leading to negative permeability enhancement. Fundamentally, brittleness and favorable original fissures/cracks in each direction are key factors affecting permeability enhancement effects. Furthermore, the degree, distribution, and density of original fissures/cracks within a coal seam vary greatly across different directions, resulting in significant differences in local permeability enhancement. Therefore, close attention should be paid to the development of original fissures/cracks and the brittleness of coal seams in different directions to provide valuable insights for selecting well type and fracturing techniques.

Due to the heterogeneous and discontinuous distribution of original fissures/cracks within the same

coal bed in practical engineering, the impact of hydro-fracturing reconstruction may vary significantly across different blocks, positions, and directions. This variability is also a key factor contributing to the complex fluctuations observed in various parameters related to on-site fracturing, drainage, and gas production. When favorable fissures/cracks are oriented at a large angle with respect to the coal seam, they are more susceptible to penetration during the hydro-fracturing process. This facilitates the formation of a voluminous fracture network and greatly enhances the overall fracturing effectiveness. Conversely, areas with inferior original fissures/cracks may exhibit a small intersection angle between these features and bedding. In such cases, compression along the bedding during hydro-fracturing can lead to closure of these features, thereby limiting or even negating any increase in permeability within the coal seams.

Although the original fissures/cracks in the same coal seams are heterogeneous and random to varying degrees, their occurrence, density, and distribution still exhibit certain regularity. When logging and coring, it is recommended to thoroughly comprehend the distribution characteristics and laws of original fissures/cracks, and take appropriate measures based on local conditions: (1) In addition to considering the direction of in-situ stress, it is essential to also consider which direction is most conducive for maximum fracture penetration between artificial fractures and the original fissures/cracks, utilizing favorable original fissures/cracks as much as possible. (2) When selecting perforation and fracturing fluid, if bedding fracture does not easily communicate with the original fissures/cracks over a large area, increasing perforation density can be considered to enhance bedding fracture for better cutting and penetration of the original fissures/cracks. (3) Special fracturing techniques such as indirect fracturing, supercritical CO_2 fracturing or temporary in-layer plugging should be appropriately employed to improve connection between hydro-fracturing cracks and inferior original fissures/cracks while forming more complex volume fractures. (4) When necessary, close coordination with surrounding coal mining should be considered. For example: arranging CBM production layer under mined coal seam where mined coal seam acts as protective layer while CBM production layer serves as "protected layer".

The process of hydro-fracturing and gas production should be closely integrated with the working face of the upper protective layer. Mining of the protective layer can effectively alleviate pressure and enhance permeability in the protected layer. This will lead to further development of a more complex and dense favorable fracture field from the original inferior fissures/cracks, ultimately creating conditions for improving fracturing effectiveness and enhancing permeability in the protected coal layer.

4. Conclusion

In order to demonstrate the permeability of coal rock before and after fracture in the Dahebian syncline area of Liupanshui coalfield, samples from the 11# coal seam were selected to prepare bedding (0°) and vertical bedding (90°) coal samples. The uniaxial compression tests were utilized to induce cracks and damage within the samples, followed by porosity testing of the coal samples before fracture and permeability testing after fracture in order to analyze the permeability enhancement effect. The evaluation also includes an evaluation of the impact of original fissures/cracks on permeability increase after fracture and exploration of mining methods. The essential findings are as follows:

(1) The initial porosity of coal samples ranges from 2.59% to 9.39%, with an average of 7.085%. There is a significant variation in porosity, attributed not only to obvious bedding but also well-developed original fissures/cracks within the coal seams, albeit with random and heterogeneous characteristics.

(2) Results from uniaxial compression tests indicate that for 0° samples, the uniaxial compressive strength ranges from 2.943 to 4.736 MPa, with an average of 4.448 MPa (Protodyakonov's coefficient f=0.4448). This suggests a relatively low overall strength characteristic of soft coal seam, with shear-splitting failure being predominant alongside some splitting failure occurrences. Conversely, for 90° samples, the uniaxial compression strength ranges from 6.184 to 15.162 MPa, with an average of 9.911 MPa (Protodyakonov's coefficient f=0.9911), indicating significantly higher strength compared to the 0° samples. This coal seam is also characterized as a relatively soft coal seam, but the main failure mode is splitting shear, and the brittleness is stronger.

(3) The permeability increasing rate in the confining pressure rising section ranges from 0.798 to 20.694 times, with an average value of 4.588 times, indicating a certain but not ideal effect on permeability increase. The increasing rate of the confining pressure decreasing section is between 0.777 and 16.939 times, with an average increment of 4.412 times. In the confining pressure rising section, the permeability increasing rate of the 90° coal samples ranges from 0.537 to 63.109 times, averaging at 9.084 times, which is close to an order of magnitude and significantly better than that of the 0° coal samples. In the confining pressure reduction section, the increasing rate ranges from 0.449 to 72 .047 times, with an average increase of 11.388 times.

(4) In locations or directions where favorable original fissures/cracks are present at a large angle with the coal seam, during hydro-fracturing, these original fissures/cracks and horizontal fractured cracks easily intersect each other, promoting the formation of volume fracturing network and greatly improving fracturing effectiveness. In logging and coring processes, it is important to fully understand the distribution characteristics and laws regarding original fissures/cracks, and make recommendations based on local conditions accordingly.

Acknowledgement

This research was supported by Guizhou Provincial Key Technology R&D Program "Research on key theories and technologies of coalbed methane development in multi-

branch horizontal Wells of high rank coal reservoirs in Guizhou Province" (NO. QianKeHeZhiCheng[2023]YiBan369) and the Guizhou Geological Exploration Fund Project (Nos. 52000021MGQSE7S7K6PRP and 52000024P0048BH101732).

References

1. Lenox, C., Kaplan, P. O. Role of natural gas in meeting an electric sector emissions reduction strategy and effects on greenhouse gas emissions. Energy Economics 60: 460-468. (2017)
2. Brauers, H. Natural gas as a barrier to sustainability transitions? A systematic mapping of the risks and challenges. Energy Rrsearch and Social Science 89: 102538. (2022)
3. Liu, W., Zhang, X., Fan, J., Li, Y., and Wang, L. Evaluation of potential for salt cavern gas storage and integration of brine extraction: Cavern utilization, Yangtze River Delta Region. Natural Resources Research 29(5): 3275-3290. (2020)
4. Nguyen, A. H. Stress state and pore pressure distribution around a horizontal wellbore within a saturated anisotropic rock with low permeability. Journal of Applied Science and Engineering 6(6): 610-618. (2023)
5. Zou, C., Yang, Z., Zhang, G., Hou, L., Zhu, R., and Tao, S. Conventional and unconventional petroleum "orderly accumulation": Concept and practical significance. Petroleum Exploration and Development 41(1): 14-30. (2014)
6. Guo, T., Xiong, L., Ye, S., Dong X., Wei, L., and Yang, Y. Theory and practice of unconventional gas exploration in carrier beds: Insight from the breakthrough of new type of shale gas and tight gas in Sichuan Basin, SW China. Petroleum Exploration and Development 50(1): 27-42. (2023)
7. Jia, C., Zheng, M., and Zhang, Y. Unconventional hydrocarbon resources in China and the prospect of exploration and development. Petroleum Exploration and Development 39(2): 139-146. (2012)
8. Tao, S., Chen, S., and Pan, Z. Current status, challenges, and policy suggestions for coalbed methane industry development in china: a review. Energy Science and Engineering 7(4): 1059-1074. (2019)
9. Zou, C., Tao, S., Han, W., Zhao, Z., Ma, W., and Li, C. Geological and geochemical characteristics and exploration prospect of coal-derived tight sandstone gas in China: case study of the Ordos, Sichuan, and Tarim Basins. Acta Geologica Sinica-English Edition 92(4): 1609-1626. (2018)
10. Wei, D., Zhao, Y., Liu, H., Yang, D., Shi, K., and Sun, Y. Where will China's shale gas industry: A scenario analysis of socio-technical transition. Energy Strategy Reviews 44, 100900. (2022)
11. Guo, X., Hu, D., Shu, Z., Li, Y., Zheng, A., and Wei, X. Exploration, development and construction in the Fuling national shale gas demonstration area in Chongqing: Progress and prospect. Natural Gas Industry 42(8): 14-23. (2022)
12. Development status of China's coalbed methane industry, future production growth rate and "13th Five-Year" target analysis. https://www.chyxx.com/industry/201902/713408.html
13. Lei, B., Qin, Y., Gao, D., Fu, X., Wang, G. F., and Zou M. Vertical diversity of coalbed methane content and its geological controls in the Qingshan syncline, western Guizhou province, China. Multi Science Publishing. (2012)
14. Sun, H., Wang, C. Damage mechanism of cement slurry to CBM reservoirs with developed fractures and cleats: A case study from eastern Yunnan and western Guizhou in China. Natural Gas Industry B 6(2): 145-150. (2019)
15. Shu, Y., Sang, S., Zhou, X., and Zhao, F. Numerical analysis of drainage rate in multi-layer coalbed methane development in Western Guizhou, Southern China. Petroleum Science and Technology 2239280. (2023)
16. Gao, D., Qin, Y., Yi, T. CBM geology and exploring-developing stratagem in Guizhou Province, China. Proceedings of the International Conference on Mining Science & Technology 1(1): 882-887. (2009)
17. Ranathunga A. S., Perera M. S. A., Ranjith P. G. Deep coal seams as a greener energy source: a review. Journal of Geophysics and Engineering 11(6), 063001. (2014)
18. Lu, P., Li, G., Huang, Z., He, Z., Li, X., and Zhang, H. Modeling and parameters analysis on a pulsating hydro-fracturing stress disturbance in a coal seam. Journal of Natural Gas Science and Engineering 6: 253-263. (2015)
19. Keshavarz, A., Yang, Y., Badalyan, A., Johnson, R., and Bedrikovetsky, P. Laboratory-based mathematical modelling of graded proppant injection in CBM reservoirs. International Journal of Coal Geology 136: 1-16. (2014)
20. Liu, W., Zhu, X., Li, L., Zhao, L., Zhou, P., Zhang, X., and Qin J. Research on the seepage properties of coal with different particle size proppant under cyclic loading. Physics of Fluids 35(4), 0143895. (2023)
21. Palmer, I. D., King, N. S., and Sparks, D. P. The character of coal fracture treatments in Oak Grove Field, Black Warrior Basin. SPE Annual Technical Conference and Exhibition, Dallas, Texas. (1991)
22. Jin, A., Li, G., and Wang, F. hydro-fracturingmethod for shallow permeability exploration of anthracite seam in Jincheng. China Coalbed Methane 02: 71-74. (1995)

23. Fredd, C. N., Olsen, T. N., and Brenize, G. Polymer-free fracturing fluid exhibits improved cleanup for unconventional natural gas well applications. SPE Eastern Regional Meeting, 15-17 September, Charleston, West Virginia. (2004)
24. Zhai, C., Li, X., and Li, Q. Research and application of coal seam pulse hydro-fracturing technology. Journal of China Coal Society 36(12): 1996-2001. (2011)
25. Huang, Q., Li, M., Li, J., Gui, Z., and Du, F. Comparative experimental study on the effects of water- and foam-based fracturing fluids on multi-scale flow in coalbed methane. Journal of Natural Gas Science and Engineering 103, 104648. (2022)
26. Duan, P., Zhang, C., Qu, C., and Wang, Z. Mechanisms of hydro-fracturing negative effect to coalbed methane seams. Journal of China Coal Society 39(S2): 447-451. (2014)
27. Wang, K., Li, B., Wei, J., and Li, P. Change regulation of coal seam permeability around hydraulic flushing borehole. Journal of Mining and Safety Engineering 30(05): 778-784. (2013)
28. Tu, M., Yuan, L., Miao, X., Liu, Z., Xu, N., and Fu, B. Study on seam deformation and permeability improved effect of pressure released mining in protective seam. Coal Science and Technology 41(01): 40-43+47. (2013)
29. Feng, W., Su, X., Wang, J., Qin, J., and Li, X. The mechanism and field test of permeability improvement by hydraulic flushing in “three-soft” and single coal seam. Coal Geology and Exploration 43(01): 100-103. (2015)
30. Xue, Y., Liu, J., Ranjith, P. G., Liang, X., and Wang, S. Investigation of the influence of gas fracturing on fracturing characteristics of coal mass and gas extraction efficiency based on a multi-physical field model. Journal of Petroleum Science and Engineering 206. (2021)
31. Cai, B., Wang, X., Jiang, T., and Lu, X. Application of hydraulic CO2 fracturing technique in coalbed gas fracturing. Natural Gas Technology (05): 40-42+94. (2007)
32. Liu, W., Zhang, Z., Fan, J., Jiang, D., Li, Z., and Chen, J. Research on gas leakage and collapse in the cavern roof of underground gas storage in thinly bedded salt rocks. Journal of Energy Storage 31: 101669. (2020)
33. Li, L., Yang, D., Liu, W., Zhang, X., Zhao, L., and Zhu, X. Experimental study on the porosity and permeability change of high-rank coal under cyclic loading and unloading. ACS Omega 34(7): 30197-30207. (2022)
34. Xia, Y., Tan, P., Wang, X., and Ren, L. Differences of fracture propagation behavior for two typical fractured formations. Natural Gas Industry B 9(3): 264-270. (2022)
35. Fan, P. H., Nie, B. S., Peng, B. Coal Permeability Study for Gas Disaster Control under Stress Paths of Three Mining Layouts. Journal of Applied Science and Engineering 20(4): 491-502. (2017)